J Mater Sci (2006) 41:7005–7010
DOI 10.1007/s10853-006-0221-6

The effect of photo-oxidation on thermal and fire retardancy of polypropylene nanocomposites

Magatte Diagne · Mamadou Gueye · Anicet Dasilva · Loic Vidal · Adams Tidjani

Received: 22 December 2004 / Accepted: 30 April 2005 / Published online: 16 September 2006

Abstract Nanocomposites of polypropylene-graft-maleic anhydride/clay were prepared by melt blending in an extruder mixer. The nanoscale dispersion of the clay in the polymer was analysed by wide-angle X-ray diffraction (XRD) and transmission electron microscopy (TEM). The results of XRD and TEM showed that the nanocomposites obtained were a kind of intercalated-delaminated structures side by side with different dominant states, depending on the clay used and on the processing conditions. The consequences of photo-oxidation on the thermal stability and fire retardant properties of the nanocomposites were investigated using thermogravimetric analysis and cone calorimetry tests. It appeared that this degradation dramatically affected the important properties of the nanocomposites. A loss of thermal stability and fire retardant performance was observed. This was ascribed to scission reactions that occurred during the oxidative degradation prior to thermal and fire tests.

Introduction

Nanocomposite technology has been the topic of several scientific papers in the last decades. This interest is due to the potential applications of nanocomposites in several areas such as [1] packaging, film barrier, automotive and so on. The starting point of its great interest occurred when the Toyota group [2] announced remarkable enhancement of polyamide-6 clay nanocomposite properties, containing only 5% clay. They found an increase of 40% in tensile strength, 68% in tensile modulus, 60% in flexural strength and 126% in flexural modulus, while the heat of distorsion temperature increases from 65 to 152 °C. Today in literature, numerous articles can be found on nanocomposites dealing with production of nanocomposites using different techniques and host polymer, thermal stability, fire retardance and permeability of nanocomposites.

The typical methods used to produce polymer nanocomposites are: intercalation of a suitable monomer followed by polymerisation, polymer intercalation from solution, and direct polymer intercalation. Intercalation of polymer melts is the most attractive method because of its ease, its environmental benignancy and cost effectiveness.

The current favourite nano-clay used is montmorillonite (MMT). The clay exists in a tactoid structure of 20–25 layers, which translates into an aspect ratio of about 10. Because of its hydrophilic nature, MMT is not compatible with most polymers; it must be modified and this is achieved by cations exchanging in between the silicate layers by usually alkyl ammonium ions. This operation increases the basal spacing reducing the attractive forces between the clay layers, that makes possible the intercalation of the polymer and/or the exfoliation of the clays platelets. Indeed, introduction of an alkylammonium surfactant may offer sufficient excess enthalpy for most polar polymers to promote the nanocomposite. In the case of non-polar polymers, an addition of a compatibilizer is requested to enhance the diffusion of polymers into clay galleries. Nanocomposites are described as intercalated or exfoliated. In the first case, the registry between the clay

M. Diagne (✉) · M. Gueye · A. Dasilva · A. Tidjani
LRNA, Faculté des Sciences et Techniques, Université Cheikh Anta Diop de Dakar, BP 5005 Dakar-Fann, Sénégal
e-mail: magdiagne@yahoo.fr

L. Vidal
Service de Microscopie Electronique, Institut de chimie des surfaces et interfaces CNRS UPR 9069, 15 Rue Jean Starky, BP 2488F-68057 Mulhouse, France

layers is maintained oppositely to the second case in which the clay layers are dispersed leading to the lost of registry. But generally, the two structures coexist with a dominant one.

Polypropylene one of the most widely used polyolefin's has simulated intensive research in order to produce polypropylene nanocomposite. Besides the effort put to optimize the production of polypropylene nanocomposites (PPCNs), it has been reported an increase of thermal stability and mechanical properties, an enhancement of fire retardancy, decrease of gas permeability. But there are few papers relating with the ageing of nanocomposites [3] and specifically the effect of ageing on the remarkable properties of these materials reported in literature. This investigation is of importance since it can be predicted that nanocomposites will probably replace the conventional material. In their future use, they could be submit to heat and/or light exposition that can alter their properties. In the following paper, investigation of the effect of photo-oxidation on the thermal stability and fire retardancy properties of PPCNs, prepared by extrusion is presented.

Experimental

Materials

The reference specimen was a commercial polypropylene containing 0.6% of maleic anhydride (designated as PP-g-MA) produced by Aldrich chemical company. As mentioned previously, the maleic anhydride plays the role of a compatibilizer to favour the melt blending between PP-g-MA and clay. Three montmorillonite (MMT) in which, different cations were used to change the hydrophilic nature of layered silicates to make them miscible with the hydrophobic character of polypropylene were experienced. In closite 30B and closite 20A supplied by Southern clay Products (Texas, USA), modification has done using a quaternary ammonium salt, methyl tallow bis two ethyl hydroxyl (MT2EtOH) and dimethydihydrogenatedtallow (2M2HT), respectively. The third, I28E from Nanocor (USA), is a natural montmorillonite ion exchanged with an octadecyl trimethyl amine (OD3MA).

Preparation of the nanocomposites

The melt compounding of PP with the modified clay was performed using an intermeshing twin-screw extruder Haake Rheomex TW100. The major processing variables were screw speed, barrel temperature profiles; they were set at 50 rpm for the first one, from 160 °C at the first barrel to 185 °C at the last barrel. The resulting material was pressed to produce plates or films with the aid of a hydraulic press equipped with two heated plates. These experimental conditions allowed the production of PPCNs with clay mass fraction of 5%. No stabilizer process was added during the melt blending operation. Samples for the cone calorimeter investigation (100 mm × 100 mm, 6 mm thick) were prepared using a hydraulic press with two heated plates (bucher plastics press KHL 100) at 165 °C and 120 bar. For the X-ray and TEM investigations, materials were pressed in a form of thin films (150–300 μm).

Instrumentation

Characterization of nanocomposites

The commun techniques that are used to evaluate the state of mixing of nanocomposites are X-ray diffraction (XRD) and transmission electron microscopy (TEM). XRD provides information on the registry between the clay layers as the polymer inserts. The second technique allows a direct observation of the state of org-MMT dispersion. A Philips X'Pert X-ray diffraction apparatus (Cu-K_α radiation, $\lambda = 0.154$ nm) operating at a generator voltage of 40 kV and a generator current of 20 mA was used for XRD data. The samples were scanned from 1.2 to 10° in 2θ at a rate of 0.3°/min. TEM was conducted on a Philips CM20 equipment at 200 kV on specimen microtomed with a LKB 8800 Ultratome III.

UV irradiation

For photo-oxidation operations, plates or bar of nanocomposites were exposed to UV light: under accelerated conditions using a SEPAP 12–24 unit that operates at 60 °C with wavelength longer than 300 nm, and under natural conditions at Dakar (Senegal) located at 17° E longitude and 15° N latitude. During the UV irradiation of thick plate, inhomogeneous degradation occurs. To obtain an exact idea of the degradation level in these plates, a profile of oxidation of the samples was performed using a Nicolet 800 FTIR spectrometer coupled to a Nic-plan microscope (128 scans summation, nominal resolution 4 cm^{-1}).

Thermal analysis

Thermogravimetric analysis (TGA) was carried out using a Mettler/Toledo TGA/SDTA 851. The TGA scans were recorded at a heating rate of 10 °C min^{-1}. This was done under air atmosphere in the temperature range of 20–600 °C to evaluate the thermal oxidation. Sample masses were set between 10 and 15 mg.

Fire resistance

The cone calorimetry was used to study fire retardancy properties. The cone calorimetry is designed to measure a range of important properties which characterize the fire behaviour of materials. It has the ability to measure ignitability, the heat release rate (HRR), the mass loss rate (MLR), the evolution of smoke and the rate of production of various gas species within 10%. These uncertainties are based on many runs in which thousands of samples have been combusted [4]. The cone measurements were performed in duplicate with a FTT, UK device. The tests were performed in a accordance with ASTM E-1354-92 at an incident flux of 50 kW/m^2, using a cone shaped heater. Exhaustion flow was set at 24 L s^{-1} and the spark was continuous until the sample ignited. The sample, in a form of plate (100 mm × 100 mm, 6 mm thick), was placed in an aluminium foil then inserted in a box with the same dimensions in the horizontal position.

Results and discussion

Characterization

Typical XRD patterns obtained from two nanocomposites specimen are presented in Fig. 1. The structure can be inferred from the position, shape and the intensity of the basal reflections in the XRD patterns.

For the XRD patterns of PP-2M2HT nanocomposites, the d_{001} peaks were broadened with low intensity and shifted towards lower angles. The diffuse nature of the peak makes it difficult to estimate accurately their *d*-spacings. These results suggest either a formation of intercalated nanocomposites or a mixed intercalated-exfoliated system (or simply a disordered system). For the PP-MT2EtOH, a small peak at higher angle is observed indicating an unexpected decrease of the *d*-spacing since the shear stress of the extruder is supposed to help dispersion of clay platelets and/or intercalation of the polymer chains. Some authors attribute this decrease to the partial decomposition of the organic alkyl ammonium modifier during processing, leading to decrease of the *d*-spacing. The loss of the ammonium salt and its replacement with a proton has been proposed to explain this observation [5]. Other authors have attributed this decrease to a collapse of the interlayer structure due to the shear forces [6]. Such structural variation could be related with the transition from a bilayer to a monolayer arrangement. In this laboratory, the oxidation has been blamed to be partially responsible of the decrease of the *d*-spacing [7].

TEM micrographs of the corresponding samples are presented in Fig. 2.

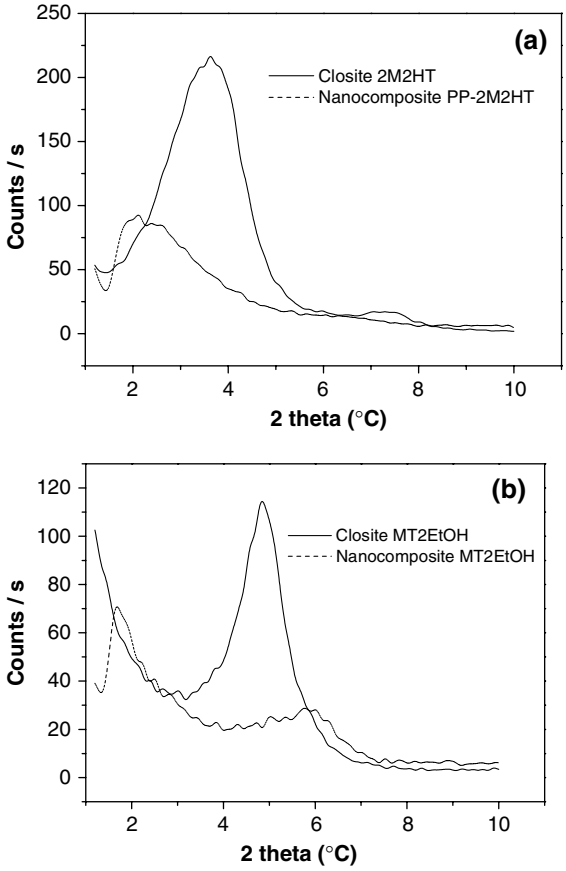

Fig. 1 XRD patterns of (**a**) Closite 20A (2M2HT) and (**b**) Closite 30B (MT2EtOH) and their nanocomposites produced by extrusion

A poor dispersion of the clay platelets and presence of tactoids is observed in Fig. 2a. The corresponding material should probably be described as an immiscible system (the dominant phase) in which some clay layers are dispersed. These are consistent with the XRD results.

In the case of the PP-2M2HT nanocomposite, a homogenous dispersion and a mixed intercalated-exfoliated system were achieved by extrusion Fig. 2b. These comfirm the diffuse nature of the peaks obtained in XRD patterns of the same specimen Fig. 1a. Hence satisfactory level of dispersion was obtained with closite 20A.

Table 1 summarizes the XRD and the TEM results of the nanocomposites produced in this work. It can be noted that PP-g-MA-OD3MA displayed an intermediary behaviour.

Oxidation profiles

It is well known that photo-oxidation of thick plates lead to heterogenous distribution of the products in the matrix attributed to poor oxygen diffusion leading to a starvation of oxygen in the bulk of the material [8]. As a result, distribution of the photoproducts within UV irradiated

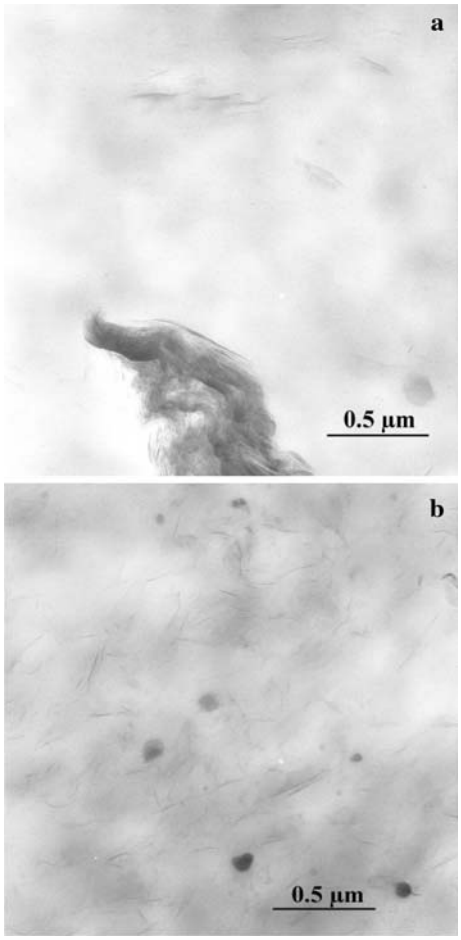

Fig. 2 TEM micrographs of PP-MT2EtOH (**a**) and PP-2M2HT (**b**) nanocomposites

specimens are requested to have an exact idea of the level of oxidation in plate. Fig. 3 presents the absorbance at 1,714 cm^{-1} as function of the distance from the exposed surface at two ageing times.

The plots were drawn from spectra recorded every 15 mm by moving the analysed area under the axis of the objective lens. After 150 h of irradiation, no significant difference is noticed from the surface to the core. On the other hand, after 300 h of UV irradiation, a higher level of oxidation is observed at the surface compared to the core of the specimens. As addition to oxygen starvation described previously, we can suspect attenuation of the light absorption within the specimen due to the presence of silicate layers. Note that the profile seems to be very dependent on the structure obtained for the nanocomposites.

Table 1 XRD and TEM results of the nanocomposites produced

Experimental	PP-2M2HT	PP-MT2ETOH	PP-OD3MA
XRD	Diffuse peak	Decrease *d*-spacing	Diffuse peak
TEM	Homogenous exfoliation	Tactoid	Tactoid exfoliation

This profile of oxidation products is probably due to the difficulty of oxygen to diffuse in the mass of specimen leading to a starvation of oxygen in the core. Some one may also suspect attenuation of the light absorption within the sample due to the presence of silicate layers. Note that the oxidation level at the surface was very dependent to the modified clay used. For instance after 300 h of UV irradiation in the SEPAP 12–24, the absorbance at 1714 cm^{-1} at the specimen surface was 0.4 for PP-g-MA, 0.65 for PP-MT2EtOH, 0.7 for PP-OD3MA and 1.85 for PP-2M2HT.

There is no doubt that the chemical changes induced by the UV degradation process may have some effect on fire properties and thermal stability of the nanocomposites. The corresponding results are presented in the next sections.

Cone calorimetry

The assessment of flammability of nanocomposites is usually performed by cone calorimetry. Cone calorimetry is designed to measure a range of important properties which characterize the fire behaviour of materials. It has the ability to measure the time to ignition (t_{ign}), the peak heat release rate (PHRR), and the time to (t_{PHRR}), the average specific extinction area (SEA), a measure of a smoke and the mass loss rate (MLR). Table 2, including all these parameters and visual observations during cone tests of the non-UV irradiated specimen, is presented below.

Looking first at the reduction in PHRR, the best has been obtained with the nanocomposite PP-2M2HT. This reduction is accompanied by a decrease of the ignition time (t_{ign}) and the t_{PHRR} without significant changes in the heat of combustion Hc, smoke yield (SEA) and carbon monoxide yield (not shown in Table 2). This indicates that the improvement of fire behaviour occurs in the solid phase and not in the gas phase.

Concerning the visual observations of the nanocomposites through the cone tests, it has been extensively described elsewhere [9]. In brief, the sample surface rapidly solidified to give a layer prior to ignition. This layer grows uniformly with the appearance of cracks that remained throughout the combustion test.

The cone tests performed on UV irradiated specimens revealed some changes in fire behaviour comparatively to non-irradiated materials. The discussion will be focussed on the PHRR, the mass loss rate and the time to ignition. The two first parameters are supposed to best described the fire behaviour of the mass of specimen, as for the ignition time, it could best inform on the state of degradation surface of samples tested.

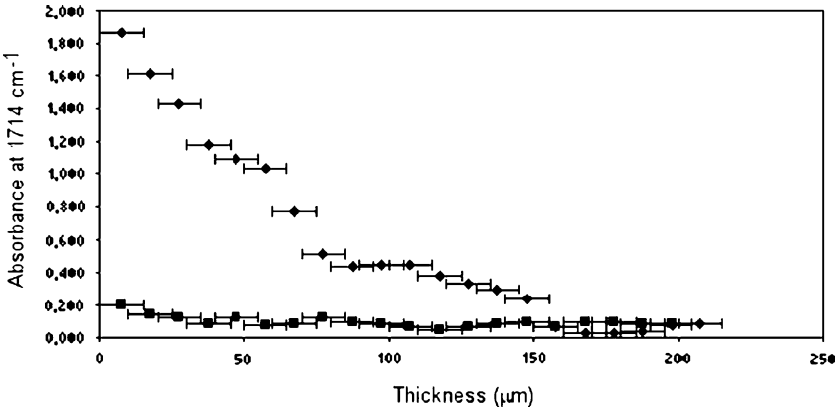

Fig. 3 Variation of absorbance at 1,714 cm^{-1} as a function of the distance from the irradiated surface in a 5 mm thick plate of PP-2M2HT nanocomposite UV-irradiated at different times of ageing in a SEPAP 12–24: (■) after 150 h, (♦) after 300 h

The general tendency drawn from Fig. 4 is that nanocomposites displayed an increase of the PHRR with the ageing time, whatever the irradiation conditions.

This result is clearly observed in Fig. 5 that depicted the heat release rate of PP-g-MA, virgin and UV-irradiated PP-2M2HT nanocomposites. As for PP-g-MA a surprising decrease of the PHRR is noticed. These changes in PHRR is accompanied, under accelerated conditions, by a decrease of the ignition time for PP-OD3MA and PP-2M2HT and, an increase of it for PP-g-MA and PP-MT2EtOH. Under natural conditions, the time to ignition (t_{ign}) decreased for PP-g-MA and PP-2M2HT and, increased for PP-OD3MA and PP-MT2EtOH.

These results show that UV irradiation has a negative influence on the fire behaviour of nanocomposites as stated by the increase of the PHRR without a significant changes in the mass loss. This could be explained by the presence of small oxidation products issue from the degradation, that are more keen to ignite. Since these oxidation products are located in the first microns of the plate, they can contribute to increase the PHRR but they cannot change significantly the fire behaviour of the bulk material. From these explanations, we should expect a decrease of the ignition time; this was the case for PP-2M2HT nanocomposites whatever the irradiation conditions. In the opposite, for the other nanocomposites, the irradiation conditions seem to play a role on (t_{ign}). The outstanding fire behaviour improvement of UV degraded PP-g-MA calls for other explanation. The decrease of its PHRR is accompanied by a decrease of its mass loss; that indicates that an improvement occurs in the bulk. This improvement is probably due to cross linking reactions that occur in the bulk because of the oxygen starvation mentioned previously. The cross linking reactions may create a compact structure which is less easily volatilizable. The question that may be risen is why this cross linking effect is not visible in UV oxidized nanocomposites. It can be blamed to the presence of clay platelets that reduces the formation of radicals by attenuating the UV lights, and also, prevents radical mobility.

Thermal degradation

The TGA curves are consistant with a single step degradation process for all samples produced. Table 3 collects the TGA data corresponding to the temperatures at which 10% and 50% degradation occur, the peak in the derivative curve and, the fraction of non-volatile material at 600 °C, referred as residue of virgin and UV degraded PPCN.

For virgin samples, it can be noted an improvement of the thermal stability of the nanocomposite compared to PP-g-MA. The mass loss is retarded with a shift of the $T_{10\%}$, $T_{50\%}$ and DTG towards the higher temperature range (up to 27, 32 and 16 °C for the PP-2M2HT). The presence of the clay, in the form of nanocomposite, exerts some positive effects on the thermal degradation. On the other hand, photo-oxidation exerts a negative effect on both PP-g-MA and the nanocomposite as stated by the decrease of the TGA data as UV irradiation increases, whatever the mode of irradiation. This effect was expected since scission reactions (that damaged the material) are involved in the photo-oxidation process. Though the surface specimen was apparently the main part of the plate to be affected by

Table 2 Cone calorimeter average data of the virgin PP-g-MA and its nanocomposites

Sample	TI (s)	PHRR (kW m^{-2}) (% reduction)	TPHRR (s)	Mean Hc (MJ/kg)	SEA	Visual observations
PP-g-MA	35	1010	294	34.66	580	Dripping
PP-OD3MA	27	609 (40)	258	38.14	667	Swelling/bubling
PP-2M2HT	29	491 (52)	211	36.52	681	Swelling/bubling
PP-MT2EtOH	26	776 (23)	295	38.92	665	Dripping

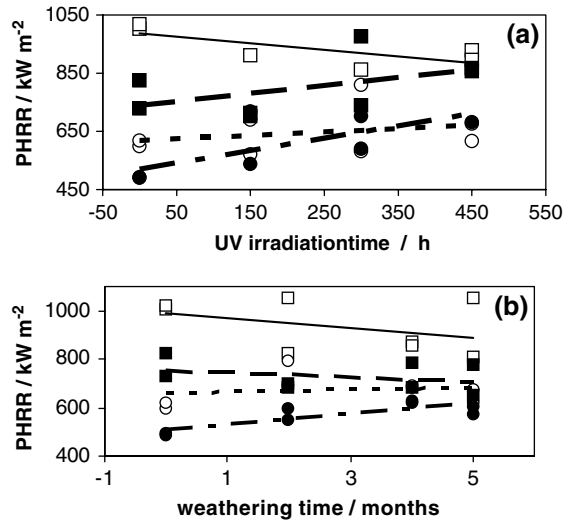

Fig. 4 PHRR changes of PP-g-MA and its nanocomposites degraded under accelerated (**a**) and natural conditions (**b**). Correspondance of symbols: PP-g-MA (□), PP-MT2EtOH (■), PP-OD3MA (○), PP-2M2HT (●)

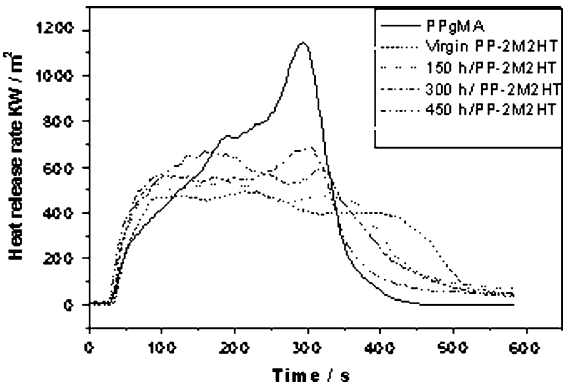

Fig. 5 The HHR variations of virgin and UV degraded PP-2M2HT nanocomposites comparatively to virgin PP-g-MA

the UV irradiation, a decrease in thermal stability is observed.

Conclusion

The true PP/clay nanocomposites exhibited improved thermal stability and fire retardancy properties at a clay loading of 5% by weight. The most interesting finding of this study was the dramatic change of these properties observed in the UV degraded nanocomposites. The onset temperatures of degradation and the PHRR decreased with aging time for nanocomposites but not the mass loss rate. This was due to weak points created in the bulk of material by the UV degradation process. On the other hand an outstanding improvement of fire properties was achieved on UV irradiated PP-g-MA. This was due to crosslinking reactions that generate a compact structure, which is less easy volatilizable.

Table 3 TGA data in air atmosphere for PP-g-MA and its nanocomposites

Samples	Time	$T_{10\%}$	$T_{50\%}$	DTG	Residue
PP-g-MA	0 h (virgin)	310	376	411	0.81
	2 months	322	389	418	0.82
	4 months	314	380	392	0.74
	300 h	311	387	415	0.844
	450 h	304	378	387	0.81
PP-OD3MA	0 h (virgin)	330 (20)	401 (24)	419 (8)	1.02
	2 months	328	401	419	1.11
	4 months	318	395	417	0.97
	300 h	312	390	409	1.10
	450 h	307	387	405	1.08
PP-2M2HT	0 h (virgin)	337 (27)	408 (32)	427 (17)	0.97
	2 months	324	401	419	1.0
	4 months	329	407	425	1.03
	300 h	328	395	412	1.00
	450 h	317	393	414	0.95
PP-MT2EtOH	0 h (virgin)	313 (4)	387 (11)	401 (–10)	1.15
	2 months	319	389	409	1.02
	4 months	322	394	412	0.93
	300 h	308	390	411	1.15
	450 h	301	388	406	1.26

Acknowledgements The authors are indebted to the Volkswagen foundation for the financial support, the Federal Institute for Research and Testing (BAM) for the cone tests, Mr. Claude da Silva from the Université de Mulhouse, France, for the X-ray measurements and, Dr. Bénédicte Mailhot from the Laboratoire de Photochimie de l'Université BP de Clermont, France, for the oxidation profile.

References

1. Revue de Sciences physiques, nanoscience, microélectronique, matériau (2004) Mai, No. 11
2. Kojima Y, Usuki A, Kawasumi M, Okada A, Fukushima Y, Kurauchi T, Kamigaito O (1993) J Mater Res 8:1185
3. Tidjani A, Wilkie CA (2001) Polym Deg Stab 74:33
4. Gilman JW, Kashiwagi T, Nyden M, Brown JET, Jackson CL, Lomakin S (1998) In: Al-Malaika S, Golovoy A, Wilkie CA (eds) Chemistry and technology of polymers additives. Blackwell Science, Oxford, pp 249–65
5. Zanetti M, Camino G, Thomann R, Mulhaupt R (2001) Polymer 42:4501
6. Kim KN, Kim H, Lee JW (2001) Polym Eng Sci 41(11):1963
7. Tidjani A, Wald O, Pohl MM, Hentschel MP, Schartel B (2003) Polym Deg Stab 82:133
8. Gradette J-L, Sinturel C, Lemaire J (1999) Polym Deg Stab 64:411
9. Tidjani A (2005) Polym Deg Stab 87:43